NANO LETTERS

pubs.acs.org/NanoLett

Letter

Optical Assessment of Tear Glucose by Smart Biosensor Based on Nanoparticle Embedded Contact Lens

Hee-Jae Jeon, Sooyeon Kim, Sijin Park, In-Kyung Jeong, Jaheon Kang, Young Ro Kim, Dong Yun Lee,* and Euiheon Chung*

Cite This: *Nano Lett.* 2021, 21, 8933−8940

Read Online

ACCESS | Metrics & More | Article Recommendations | Supporting Information

ABSTRACT: Diabetes is a disease condition characterized by a prolonged, high blood glucose level, which may lead to devastating outcomes unless properly managed. Here, we introduce a simple camera-based optical monitoring system (OMS) utilizing the nanoparticle embedded contact lens that produces color changes matching the tear glucose level without any complicated electronic components. Additionally, we propose an image processing algorithm that automatically optimizes the measurement accuracy even in the presence of image blurring, possibly caused by breathing, subtle movements, and eye blinking. As a result, using *in vivo* mouse models and human tear samples we successfully demonstrated robust correlations across the glucose concentrations measured by three different independent techniques, validating the quantitative efficacy of the proposed OMS. For its methodological simplicity and accessibility, our findings strongly support that the innovation offered by the OMS and processing algorithm would greatly facilitate the glucose monitoring procedure and improve the overall welfare of diabetes patients.

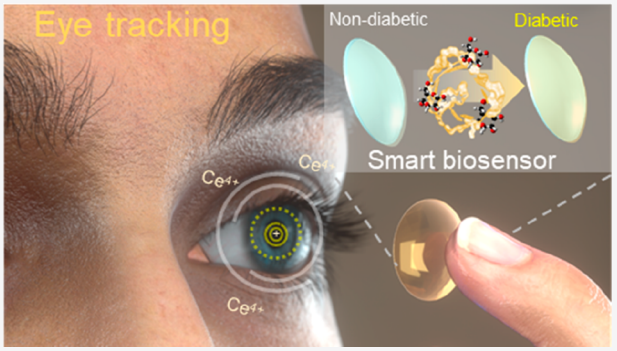

KEYWORDS: *optical monitoring system (OMS), nanoparticle embedded contact lens (NECLs), image processing algorithms, tear glucose*

Diabetes is one of the major diseases responsible for chronic illness and frequent mortality.[1−5] The prolonged elevation of glucose level in body fluids such as blood and urine substantially increases the risk of cardiovascular diseases, while other grim complications including diabetic retinopathy, diabetic nephropathy, and diabetic neuropathy, and long-term cognitive deficit.[5−10] Early diagnosis and proper glycemic management are crucial to control and prevent further progression and complications. In modern management of diabetes, conventional point-of-care glucose monitoring systems and blood glucose self-testing (BGST) are usually recommended. However, since both methods require pricking a finger to obtain a small amount of blood for analysis,[11,12] the patient's compliance with frequent, routine testing up to eight times a day is usually low due to the involved discomfort and procedural inconveniences, further raising the risk of feared complications.[13]

On the other hand, tear fluid has been known to reflect the elevated glucose concentration in the blood of diabetes patients and is suggested as a source of test medium.[14,15] Compared to the traditional blood test, evaluating the tear fluid glucose level offers a noninvasive option for continuous *in vivo* and in situ monitoring. Technically for this purpose, a number of measurement methods employing either electric sensors or optical arrangements have been proposed and widely investigated.[16−19] In particular, continuous monitoring of tear fluids has been frequently performed using the electronic glucose sensors; however, the sensors in the device are not typically biocompatible, thus limiting the *in vivo* measurement. Moreover, electric drifts in the sensor response constantly require frequent calibrations with fresh blood samples. Ultimately, unfavorable drawbacks in the construction of the electric glucose system such as bulky detector, complicated fabrication process, and excessive electrical components warrant major improvement of the device structure and measurement concept.[20,21]

Regarding the current optical technologies in the broad sense, two detection concepts, one based on surface plasmon resonance (SPR) and the other on fluorescence resonance energy transfer (FRET), are widely accepted and studied for designing quantification strategies of the tear glucose concentration.[22,23] These techniques are typically based on evaluating color changes in an optical indicator that responds

Received: May 19, 2021
Revised: August 12, 2021
Published: August 20, 2021

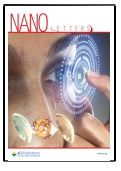

https://doi.org/10.1021/acs.nanolett.1c01880
Nano Lett. 2021, 21, 8933−8940

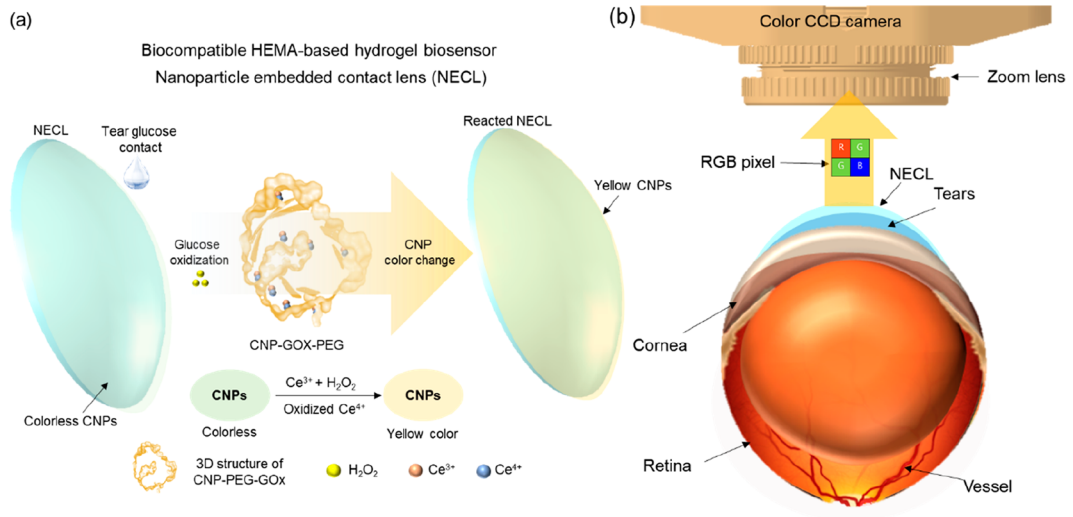

Figure 1. Schematic illustration of colorimetric NECL and optical monitoring system. (a) NECL color was changed to yellow (colorless Ce^{3+} to yellow Ce^{4+}) as it exposed to tear depending on glucose concentration. (b) A color CCD camera with a zoom lens for the demagnification (0.45×) record NECL surface color change (RGB). CNPs, cerium oxide nanoparticles; PEG, polyethylene glycol; GOx, glucose oxidase; HEMA, hydroxyethyl methacrylate; H_2O_2, hydrogen peroxide.

to the activation of fluorescently labeled enzymes by glucose. However, the approaches usually require an additional, high-power light source to consistently estimate the tear glucose concentration from the contact lens, which may cause damage to the cornea.[13,24] Furthermore, the measurement accuracy and clinical practicality of these techniques can be easily hampered by their high sensitivity to motion, a requirement of a long calibration process, and short lifetime of fluorophores by degradation.[24] Because of such demerits, optical techniques have been deemed inefficient and unsuitable for monitoring the tear glucose level despite the potential *in vivo* and in situ advantages.[25]

To improve practical measurement of the tear glucose concentration, we devised a unique, clinically feasible optical quantification method based on the nanoparticle embedded contact lenses (NECLs), therefore eluding the imitations as mentioned earlier. In this letter construct, a simple camera-based optical monitoring system (OMS) was designed and built using NECL in Figure 1b. This colorimetric contact lens produces a unique color change depending on the tear glucose concentration without any complicated electrical components and high power light sources. Additionally, we developed image processing algorithms that maximize the measurement accuracy even in image blurring due to motion artifact. Along with such improvements, the central objective of the current research was to facilitate both sampling and testing of the diabetes assay medium through the use of tear fluid. Experimental validations were performed with collected human tear samples and murine subjects *in vivo*. In particular, in situ glucose monitoring was performed in the eyes of awake (transgenic and normal) and anesthesia mice (inhalant and injectable anesthesia), which demonstrated *in vivo* measurement accuracy of the proposed OMS as well as its clinical feasibility. These innovative features provided by the OMS with its processing algorithm would greatly benefit patients by enabling the near real-time visualization of the blood glucose level and by significantly alleviating pain, discomfort, and other inconveniences involved with the traditional testing methods of diabetes.

Colorimetric contact lens of NECLs consisted of cerium oxide nanoparticles (CNPs), glucose oxidase (GOx), and polyethylene glycol (PEG) complex. NECLs oxidize tear glucose to produce hydrogen peroxide (H_2O_2), the NECL's color turns yellowish after reacting with Ce^{3+} and H_2O_2, and it oxidized Ce^{4+}, as shown in Figure 1a. NECL of HEMA-based contact lens was fabricated with 105 μL of ethylene glycol dimethacrylate (EGDMA), 34 μL of methacrylic acid (MAA), and 17 μL of photoinitiator mixed with 4 mL of 2-hydroxyethyl methacrylate (HEMA). CNP-PEG-GOx complexes, prepared based on the previous methods,[26] were added to the HEMA-based contact lens solution and sonicated for dispersion, subsequently filling a plastic curvature shape mold and being polymerized by UV illumination (365 nm, 15 mW/cm^2) for 30 min. NECLs are immersed in distilled water for cleaning and stored in 0.9% NaCl at 4 °C. The CNPs are known to undergo a reversible transformation between Ce^{4+} and Ce^{3+} in photocatalytic applications.[27,28] Since the reverse chemical reaction of CNPs occurs slowly, the NECLs were used for identifying forward reaction (increment) only rather than dynamic glucose estimation. In addition, the biocompatibility of NECLs was tested with human umbilical vein endothelial cells (HUVECs) and human corneal epithelial cells (HCECs) using the Cell Counting Kit-8 (CCK; Dojindo, Japan).[29,30] The NECLs were exposed for 24 h in an incubator (at 37 °C, 5% CO_2) and showed no cytotoxicity to HUVECs and HCECs in Supporting Information Figure S9. To improve the visibility through the NECLs with wearing, we created center-transparent NECLs in the shape of a doughnut with a clear central field of view as shown in Supporting Information Figure S10.

The experimental configuration for the measurement of tear glucose concentration is shown in the Supporting Information (Figure S1a). After the animal is placed on the heating pad in this setup, the white light LED (MWWHL4, Thorlabs Inc., U.S.A.) with a diffuser was used for uniform illumination. A CCD camera (QIClick, Qimaging, U.S.A.) with a demagnification zoom lens (MVL6 × 12Z, Thorlabs, U.S.A.) was used to record the NECL's color variation for 5 min. We also modified the system for the human tear glucose test. White light LED

https://doi.org/10.1021/acs.nanolett.1c01880
Nano Lett. 2021, 21, 8933−8940

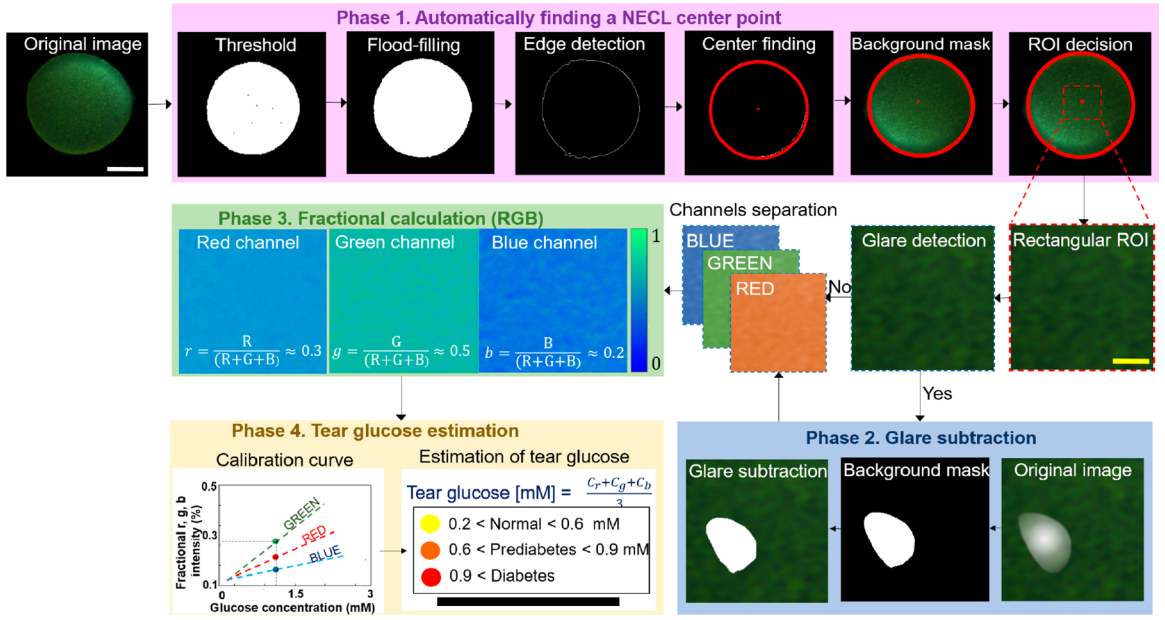

Figure 2. The overall process to estimate the colorimetric NECL color change in response to tear glucose concentration. The flowchart consisted of four steps: automatically finding a lens center point, glare subtraction, fractional calculation of R, G, B color, and tear glucose measurement. ROI, region of interest; r,g,b, fractional red, green, blue intensity; R, G, B, RED, GREEN, BLUE channel of an image; Cr,g,b, estimated tear glucose concentration. White scale bar, 1 mm; yellow scale bar, 300 μm.

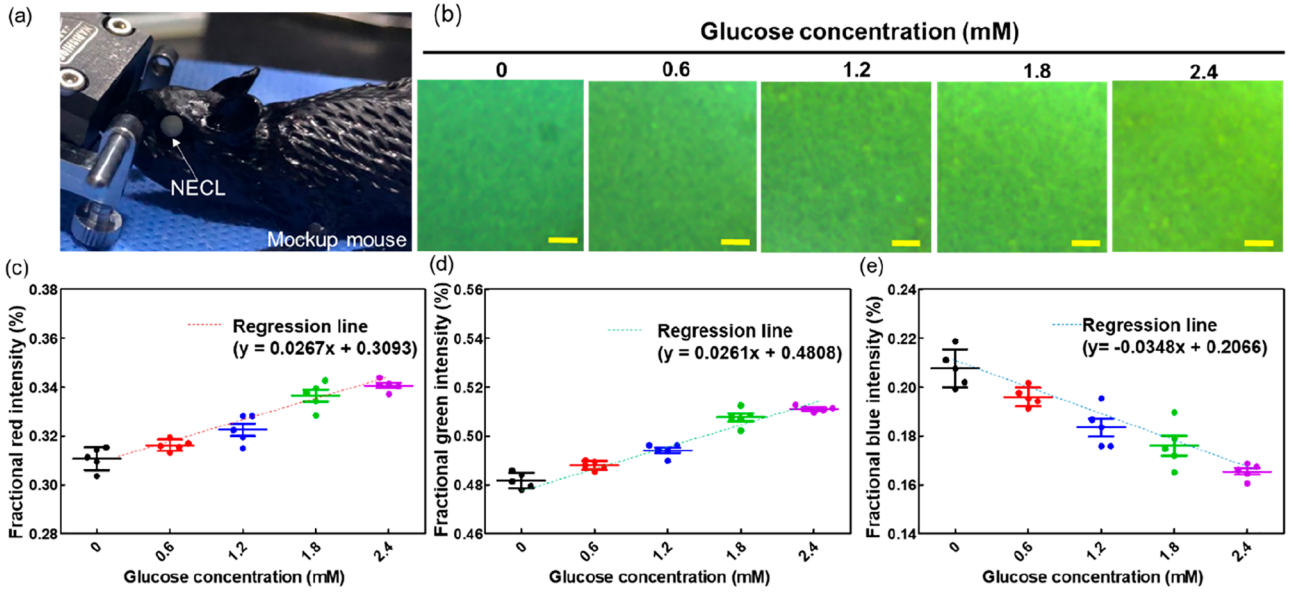

Figure 3. The calibration curve for the estimation of tear glucose concentration using fractional RGB intensities. (a) The NECLs being wearied mockup mouse eyes and monitored NECLs color. (b) The ROI color of NECLs changed to yellow as glucose concentrations were increased. The fractional RGB intensities were calculated at the different glucose concentrations (0–2.4 mM). We computed from calibration data by a linear regression line to estimate tear glucose concentration. The center of the dotted line with red, green, blue colors inside panels (c–e) indicates the regression line from the mean value. Scale bar: 200 μm (n = 5).

with a diffuser illuminates uniformly on NECLs surface placed on the three-axis stage for the human tear glucose test.

For the monitoring a unique color change of NECLs depending on the tear glucose concentration, we defined fractional RGB intensities to normalize the total signal from each channel to minimize the effect of illumination conditions. The signal variation in each color channel is minimized between the original and the fractional channel (Supporting Information Figure S3). The relative variability in the original and fractional channels are 8.92, 9.62, 11.88% for R, G, B channel and 1.72, 0.62, 3.95% for r, g, b channel, respectively. In each channel, calibration curves were computed from the calibration data by a linear regression line, $y = a + bx$, as shown in Figure 3c–e. Note that the slope of the calibration curve was positive in the red and green channels while it was negative in the blue channel. The mean fractional blue intensity difference was more prominent than the mean of fractional green and red intensity because blue has a complementary color relationship with yellow.[31] The resultant glucose concentration was estimated by the arithmetic mean of those from the three

https://doi.org/10.1021/acs.nanolett.1c01880
Nano Lett. 2021, 21, 8933–8940

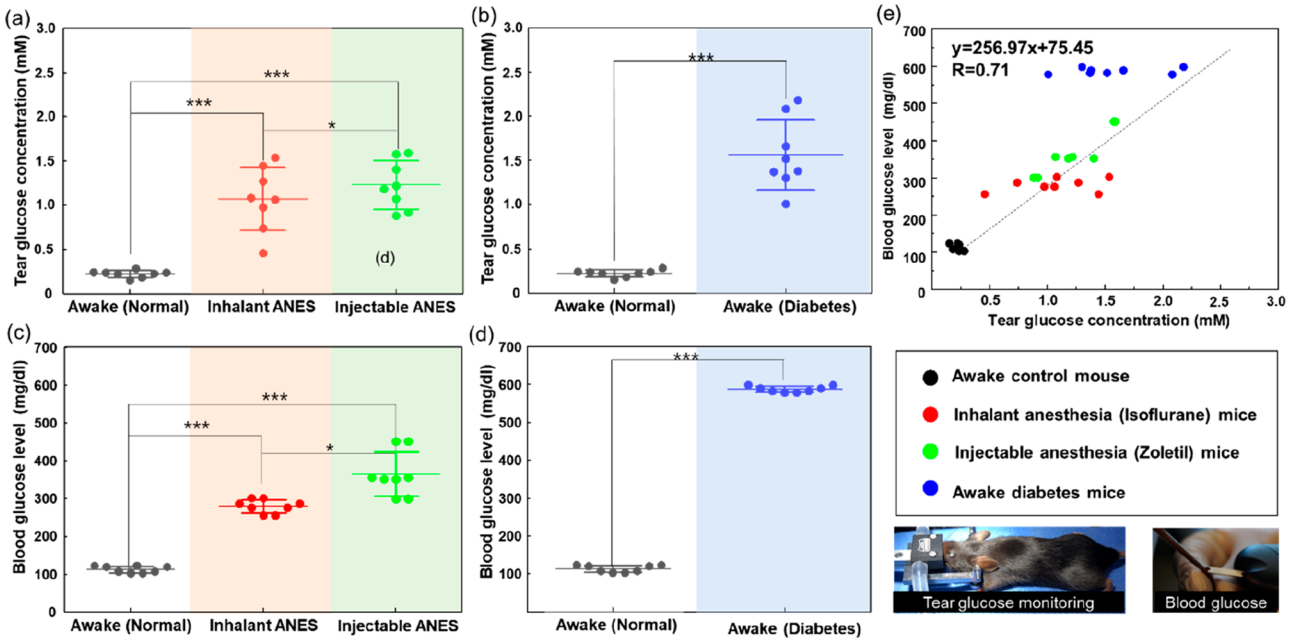

Figure 4. Analysis of estimated tear and blood glucose concentration between awake (normal and diabetic) and anesthesia mice (isoflurane and Zoletil). The comparison results show the difference of tear and blood glucose concentration in normal, inhalant ANES with isoflurane, injectable ANES with Zoletil, and transgenic diabetic mice (a–d). (e) We computed the linear correlation between estimated tear and blood glucose concentrations. (ANES: anesthesia; black dots, control mouse; red dots, anesthesia from isoflurane; green dots, anesthesia from Zoletil; blue dots, transgenic diabetic mice) (n = 8), *indicates p 0.05, ** p < 0.01, and *** indicates p < 0.001.

channels based on fractional RGB intensities. In addition, we investigated the NECL's color variation at low glucose concentrations (0.001, 0.01, and 0.1 mM). A meaningful colorimetric change was confirmed at the 0.1 mM by the optical monitoring system (p < 0.01 compared to 0 mM) as shown in Supporting Information Figure S7. The calibration curve performance for the low glucose detection was estimated by calculating linear regression for a range of 0.1−0.6 mM with 0.1 mM interval. Two different linear regression lines were nearly overlapped (Supporting Information Figure S8a−c), and the mean of estimated glucose difference was ±0.005 mM in 50 trials (Supporting Information Figure S8d).

With awake mice, their eyes are not always stationary during the image recording process. Even though we fixed the mouse head on a holder, the NECL images could shake due to breathing, body fluctuation, or eye blinking. To address this, we developed an algorithm to track the NECL in the eye image frames automatically (Supporting Information Movie S1), which had an exposure time of 0.3 s. The algorithm discarded images when the NECL was partially occluded or not visible during real-time image analysis (Figure 2). After removing unnecessary frames, the NECL center was automatically found, and a surrounding region of interest (ROI) was selected with a size of 150 × 150 pixels or roughly 1 mm^2. Also, a glare subtraction was applied if there were saturated pixels within the ROI. The color ROI images were then separated into three channels (Red, Green, and Blue) that provided fractional RGB intensities. The calibration curve between the glucose concentration and the fractional RGB intensities was plotted at a different glucose concentration in Figure 3ab. This calibration was used to estimate tear glucose concentration. We used 20 min of NECL reaction time to allow the cerium nanoparticles to fully diffuse throughout the hydrogel before the optical monitoring system assessed tear glucose concentration.

In the preclinical animal test, we estimated tear glucose concentration between awake groups (normal mice and transgenic diabetic mice) and anesthesia groups (inhalant and injectable) shown in Figure 4. Tear glucose concentration was higher in the anesthesia and diabetic mouse groups than in the control groups. The tear glucose concentration in each group was calculated by the average tear glucose concentration for 5 min, as shown in the Supporting Information (Supporting Information Figure S1b). The tear glucose concentration for normal mice without anesthesia was 0.24 ± 0.03 mM, and the tear glucose concentration for injectable (Zoletil) method, inhalant anesthetics (isoflurane), and transgenic diabetic mouse were 1.07 ± 0.33, 1.23 ± 0.25, and 1.56 ± 0.37 mM, respectively in Figure 4a−d. There was a strong correlation, R = 0.71, between tear and blood glucose obtained from 32 animals (eight per group) in Figure 4e. The anesthetic agents, Zoletil and isoflurane, have been reported to increase blood glucose during the anesthesia as they are known to suppress insulin secretion.[32,33] The blood and tear glucose concentration under Zoletil anesthesia was higher than isoflurane anesthesia mice in Figure 4a,c, which may depend on the depth of anesthesia.[34,35] In transgenic diabetic mice, blood glucose concentrations were relatively high (550−600 mg/dL) and tear glucose also showed a similar trend with relatively higher variation in Figure 4b−e. However, the relatively high variation of tear glucose concentration might be due to inherent variation among individuals and repeatability issues during the fabrication process of NECL.

On the other hand, in animal experiments we observed an increase in blood glucose levels over time in the restrained group for awake measurement (Supporting Information Figures S5 and S6), potentially due to increased stress levels. Also, we confirmed that tear glucose concentrations were slightly increasing in restrained animals (Supporting Information Figure S1b). Besides, the accuracy can be improved by

https://doi.org/10.1021/acs.nanolett.1c01880
Nano Lett. 2021, 21, 8933−8940

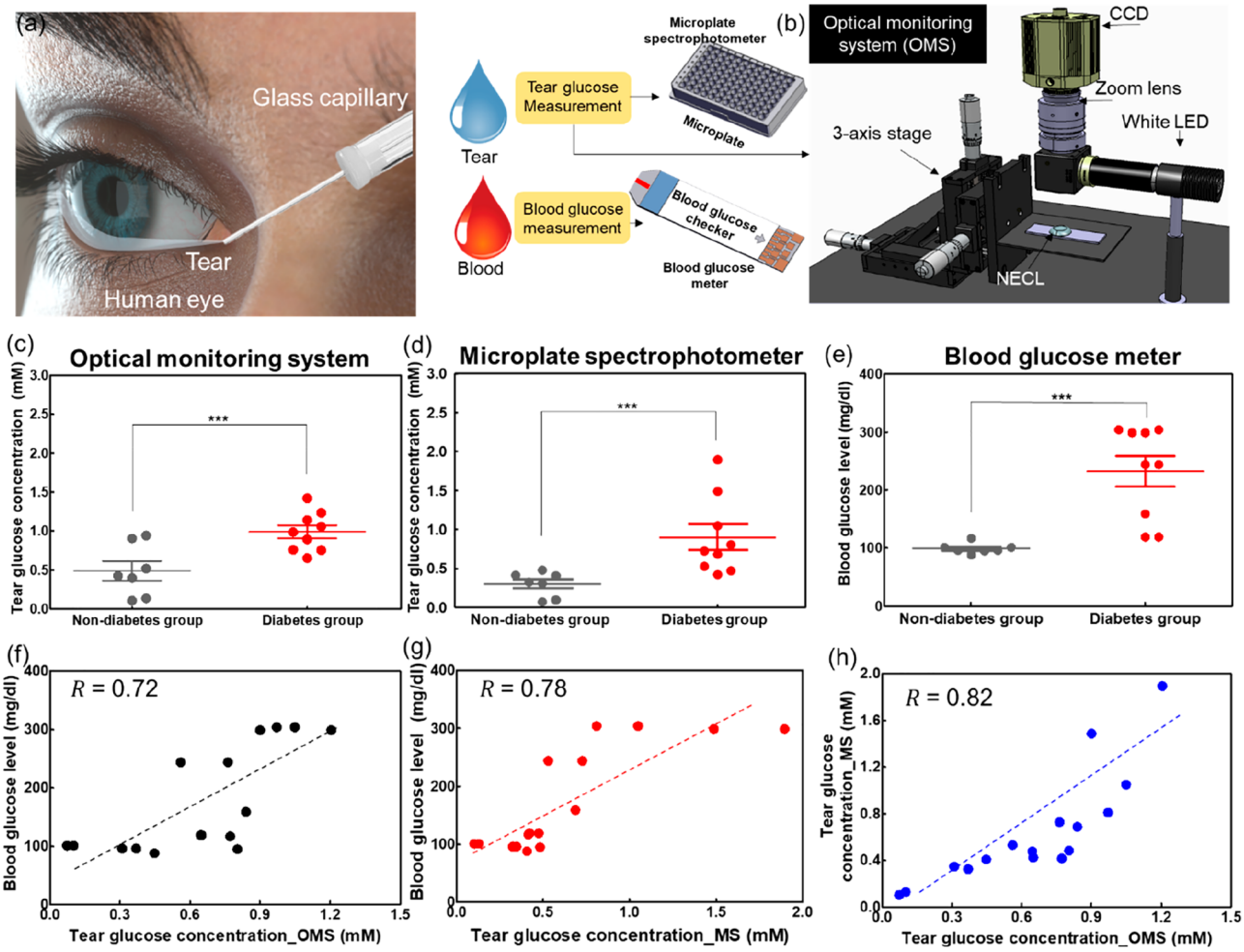

Figure 5. Analysis of human tear and blood glucose concentration between healthy subjects and diabetic patients with an optical monitoring system, blood glucose meter, and microplate spectrophotometers. (a) Human tears were collected by microcapillary glass tube from lid margin of eyes with 5−10 μL volumes after measuring blood glucose concentration by finger stick. (b) The optical monitoring system consisted of a CCD camera, a demagnification zoom lens, a white LED, and a three-axis stage. (c−e) Human tear glucose concentrations were estimated by OMS and MS after measuring the blood glucose concentration. (f−h) The linear correlations were computed among OMS, MS, and blood glucose meter. MS, microplate spectrophotometers; OMS, optical monitoring system, (n = 16), *** indicates $p < 0.001$.

postprocessing and continuous autotracking algorithm by filtering out blurred images. Moreover, algorithms have been serialized using only a single core from a quadcore CPU (Intel i7-8700); it is relatively fast and currently takes approximately 0.5 s to estimate tear glucose concentration. This postprocessing speed is enough to apply smartphone-based health care as compared to previous research results.[36]

In the clinical test, after collecting human tears with a capillary glass tube, we estimated tear glucose concentration using optical monitoring system (OMS), microplate spectrophotometer (MS), and blood glucose meter between the diabetic patients and the healthy subjects, as shown in Figure 5a,b. Tear glucose concentration by OMS and MS was increased in diabetic patients than in the healthy subjects. Estimated tear glucose concentration of healthy subjects and diabetic patients were 0.42 ± 0.25 and 0.84 ± 0.21 mM in OMS, respectively, and 0.31 ± 0.13 and 0.89 ± 0.46 mM in MS, respectively, in Figure 5c−e. The blood glucose level for healthy subjects and diabetic patients were 99.14 ± 8.34 and 232.3 ± 74.91 mg/dL, respectively. We plotted three correlations to investigate the relationship among three different methods (blood glucose, tear glucose with OMS, and tear glucose with MS) along with linear regression lines as shown in Figure 5f−h. The blood glucose meter has a moderately positive correlation with both OMS and MS (R = 0.72, and R = 0.78, respectively. The OMS based on NECL and MS have a strong positive linear correlation with R = 0.82. In previous studies, tear glucose levels were higher in diabetic patients than in healthy subjects.[7,14,37] Our data with clinical samples showed a similar tendency between healthy subjects (0.42 ± 0.25 mM) and diabetic patients (0.84 ± 0.21 mM) in Figure 5c. Clinically, the detection of hypoglycemia is also of high importance for diabetes mellitus patients since low blood glucose levels give rise to serious complications often requiring emergency care. Our benchtop study demonstrated the technical feasibility of the tear glucose quantification below 0.6 mM with the lowest detection limit of 0.1 mM (see Supporting Information Figures S7 and S8). The observation implicates the applicability of the current technique in detection of hypoglycemia. Although the resolving power likely requires improvement with further *in vivo* validations, our study shows the prospect of wide range determination of the tear glucose concentration.

https://doi.org/10.1021/acs.nanolett.1c01880
Nano Lett. 2021, 21, 8933−8940

We also directly compared estimated tear glucose concentration with the microplate spectrophotometer (MS) method, which was known as a precise way of baseline tear glucose measurement using a glucose assay kit. We confirmed a significant correlation (R = 0.82) with OMS and MS in Figure 5f. However, while the estimated tear glucose concentration between OMS and MS displayed a clear linear correlation, correlation with blood glucose meter shows relatively low (R = 0.72) in Figure 5g. This could be due to intrinsic tear glucose differences among test animals[38,39] and temporal mismatch of the dynamics of glucose concentrations between tear and blood.[32] Human tear glucose concentrations in situ were indirectly estimated from the collected human tear samples. The future direction would be applying this technique to measure the tear glucose of human subjects while wearing the NECL. This will be enabled by a smartphone or hand-held optical monitoring device with optimized image processing. Thus, the practical application of this method warrants further investigation with real-life environmental conditions such as ambient lighting and iris color.

In summary, we developed a simple camera-based optical monitoring system and an image processing algorithm to estimate tear glucose concentration based on the color changes in nanoparticle embedded contact lenses. The device provides a simple means for low-cost, quantitative, and tear glucose concentration monitoring. Evaluation of the biosensor used for tear glucose measurement, NECLs, were successfully confirmed with experimental testing of both human tear samples and *in vivo*, *in situ* animal models. The present approach provides a significant step forward in the development of a fully automated instrument for tear glucose monitoring in diabetes patients.

■ ASSOCIATED CONTENT

Supporting Information

The Supporting Information is available free of charge at https://pubs.acs.org/doi/10.1021/acs.nanolett.1c01880.

NECL was automatically tracked by finding the center position even in the presence of image shaking; overall working flow to calculate fractional r, g, b intensities; optical monitoring system to estimate tear glucose concentration for mice; comparison of fractional r, g, b intensities between artificial tear solution and deionized water; comparison of image processing between the original and fractional channels; confirmation of NECL color change by comparing fractional r, g, b intensities at different H_2O_2 concentrations; measurement of blood glucose concentration with normal and transgenic mice; measurement of blood glucose concentration with anesthesia mice (isoflurane and Zoletil); measurement of the limit of detection (LOD) at the low glucose concentrations; estimation of curve fitting at the low glucose concentration with linear regression; cytotoxicity of the NECLs; transmittance measurement of center-transparent NECLs; gender, age, and diabetes status of mice used for tear and blood glucose measurements; gender, age, and diabetes status of human subjects used for tear and blood glucose measurements (PDF)

Video of algorithm tracking the NECL in the eye image frames automatically (MP4)

Video of original image, processed image, and normalized cropped image (MP4)

■ AUTHOR INFORMATION

Corresponding Authors

Dong Yun Lee − *Department of Bioengineering, College of Engineering, and BK FOUR Biopharmaceutical Innovation Leader for Education and Research Group, and Institute of Nano Science and Technology (INST), Hanyang University, Seoul 04763, Republic of Korea; Elixir Pharmatech Inc., Seoul 04763, Republic of Korea;* orcid.org/0000-0001-7691-0447; Email: dongyunlee@hanyang.ac.kr

Euiheon Chung − *Department of Biomedical Science and Engineering, Gwangju Institute of Science and Technology (GIST), Gwangju 61005, Republic of Korea; AI Graduate School, GIST, Gwangju 61005, Republic of Korea; Department of Physics and Photon Science, GIST, Gwangju 61005, Republic of Korea;* orcid.org/0000-0002-3326-6927; Email: ogong50@gist.ac.kr

Authors

Hee-Jae Jeon − *Department of Biomedical Science and Engineering, Gwangju Institute of Science and Technology (GIST), Gwangju 61005, Republic of Korea; Weldon School of Biomedical Engineering, Purdue University, West Lafayette, Indiana 47907, United States*

Sooyeon Kim − *Department of Biomedical Science and Engineering, Gwangju Institute of Science and Technology (GIST), Gwangju 61005, Republic of Korea*

Sijin Park − *Department of Bioengineering, College of Engineering, and BK FOUR Biopharmaceutical Innovation Leader for Education and Research Group, and Institute of Nano Science and Technology (INST), Hanyang University, Seoul 04763, Republic of Korea; Elixir Pharmatech Inc., Seoul 04763, Republic of Korea*

In-Kyung Jeong − *Department of Endocrinology and Metabolism, Kyung Hee University Hospital at Gangdong, Kyung Hee University School of Medicine, Seoul 02447, Republic of Korea*

Jaheon Kang − *Department of Endocrinology and Metabolism, Kyung Hee University Hospital at Gangdong, Kyung Hee University School of Medicine, Seoul 02447, Republic of Korea*

Young Ro Kim − *Department of Radiology, Harvard Medical School, Boston, Massachusetts 02115, United States; Athinoula A. Martinos Center for Biomedical Imaging, Massachusetts General Hospital, Charlestown, Massachusetts 02129, United States*

Complete contact information is available at: https://pubs.acs.org/10.1021/acs.nanolett.1c01880

Author Contributions

H.J.J., D.Y.L., and E.C. developed the experimental design and worked on the optical measurements and NECL developments. H.J.J., S.Y.K., S.J.P., and E.C. conducted the analyses. H.J.J., Y.R.K., D.Y.L. and E.C. mainly wrote the manuscript. I.K.J. and J.K. conducted clinical tests. D.Y.L and EC directed the overall research. All authors have given approval to the final version of the manuscript.

Notes

The authors declare no competing financial interest.

■ ACKNOWLEDGMENTS

This research was supported by the GIST Research Institute (GRI) grant funded by GIST in 2021, and the 2021 Joint

Research Project of Institutes of Science and Technology, a grant from the National Research Foundation of Korea (NRF) funded by the Korean government (MEST) (NRF-2019R1A2C2086003), the Brain Research Program through the NRF funded by the Ministry of Science, ICT & Future Planning (NRF-2017M3C7A1044964), the Korea Medical Device Development Fund grant funded by the Korea government, the Ministry of Science and ICT, the Ministry of Trade, Industry and Energy, the Ministry of Health & Welfare, the Ministry of Food and Drug Safety (Project Number: 1711138096, KMDF_PR_220200901_0076), Korea Health Technology R&D Project through KHIDI, funded by the Ministry of Health & Welfare (HI19C1077000019), and partially supported by National Research Foundation of Korea (NRF) funded by the Ministry of Science, ICT & Future Planning (NRF-2015M3A9E2030125 and NRF-2020R1A2C3005834).

■ ABBREVIATIONS

OMS, optical monitoring system; NECLs, nanoparticle embedded contact lens; CNPs, cerium oxide nanoparticles; GOx, glucose oxidase; EGDMA, ethylene glycol dimethacrylate; MAA, methacrylic acid; HEMA, 2-hydroxyethyl methacrylate; ROI, region of interest; H_2O_2, hydrogen peroxide; MS, microplate spectrophotometer

■ REFERENCES

(1) Mellitus, D. Diagnosis and classification of diabetes mellitus. *Diabetes Care* **2005**, *28*, S37.
(2) Mayer, C.; Siems, W.: Diabetes mellitus. In *100 Krankheitsbilder in der Physiotherapie*; Springer, 2011; pp 42−43.
(3) Georgiou, H. M.; Lappas, M.; Georgiou, G. M.; Marita, A.; Bryant, V. J.; Hiscock, R.; Permezel, M.; Khalil, Z.; Rice, G. E. Screening for biomarkers predictive of gestational diabetes mellitus. *Acta Diabetol.* **2008**, *45*, 157−165.
(4) Vestergaard, P.; Rejnmark, L.; Mosekilde, L. Relative fracture risk in patients with diabetes mellitus, and the impact of insulin and oral antidiabetic medication on relative fracture risk. *Diabetologia* **2005**, *48*, 1292−1299.
(5) Biessels, G.-J.; Kappelle, A.; Bravenboer, B.; Erkelens, D.; Gispen, W. Cerebral function in diabetes mellitus. *Diabetologia* **1994**, *37*, 643−650.
(6) Boulton, A. J. M.; Vinik, A. I.; Arezzo, J. C.; Bril, V.; Feldman, E. L.; Freeman, R.; Malik, R. A.; Maser, R. E.; Sosenko, J. M.; Ziegler, D. Diabetic neuropathies: a statement by the American Diabetes Association. *Diabetes Care* **2005**, *28*, 956−962.
(7) Baca, J. T.; Finegold, D. N.; Asher, S. A. Tear glucose analysis for the noninvasive detection and monitoring of diabetes mellitus. *ocular surface* **2007**, *5*, 280−293.
(8) Wilkinson, C.; Ferris, F. L., III; Klein, R. E.; Lee, P. P.; Agardh, C. D.; Davis, M.; Dills, D.; Kampik, A.; Pararajasegaram, R.; Verdaguer, J. T. Proposed international clinical diabetic retinopathy and diabetic macular edema disease severity scales. *Ophthalmology* **2003**, *110*, 1677−1682.
(9) Wilmot, E. G.; Edwardson, C. L.; Achana, F. A.; Davies, M. J.; Gorely, T.; Gray, L. J.; Khunti, K.; Yates, T.; Biddle, S. J. Sedentary time in adults and the association with diabetes, cardiovascular disease and death: systematic review and meta-analysis. *Diabetologia* **2012**, *55*, 2895−2905.
(10) Boulé, N. G.; Kenny, G. P.; Haddad, E.; Wells, G. A.; Sigal, R. J. Meta-analysis of the effect of structured exercise training on cardiorespiratory fitness in Type 2 diabetes mellitus. *Diabetologia* **2003**, *46*, 1071−1081.
(11) Blair, M. Diabetes Mellitus Review. *Urologic nursing* **2016**, *36*, 27.
(12) Ding, S.; Schumacher, M. Sensor monitoring of physical activity to improve glucose management in diabetic patients: a review. *Sensors* **2016**, *16*, 589.
(13) Lee, H.; Hong, Y. J.; Baik, S.; Hyeon, T.; Kim, D. H. Enzyme-based glucose sensor: from invasive to wearable device. *Adv. Healthcare Mater.* **2018**, *7*, 1701150.
(14) Lane, J. D.; Krumholz, D. M.; Sack, R. A.; Morris, C. Tear glucose dynamics in diabetes mellitus. *Curr. Eye Res.* **2006**, *31*, 895−901.
(15) Shakeel, P. M.; Baskar, S.; Dhulipala, V. S.; Jaber, M. M. Cloud based framework for diagnosis of diabetes mellitus using K-means clustering. *Health information science and systems* **2018**, *6*, 1−7.
(16) Heller, A.; Feldman, B. Electrochemical glucose sensors and their applications in diabetes management. *Chem. Rev.* **2008**, *108*, 2482−2505.
(17) Bruen, D.; Delaney, C.; Florea, L.; Diamond, D. Glucose sensing for diabetes monitoring: recent developments. *Sensors* **2017**, *17*, 1866.
(18) Ku, M.; Kim, J.; Won, J. E.; Kang, W.; Park, Y. G.; Park, J.; Lee, J. H.; Cheon, J.; Lee, H. H.; Park, J. U. Smart, soft contact lens for wireless immunosensing of cortisol. *Science advances* **2020**, *6*, eabb2891.
(19) Kim, J.; Cha, E.; Park, J. U. Recent advances in smart contact lenses. *Advanced Materials Technologies* **2020**, *5* (1), 1900728.
(20) So, C.-F.; Choi, K.-S.; Wong, T. K.; Chung, J. W. Recent advances in noninvasive glucose monitoring. *Med. Devices: Evidence Res.* **2012**, *5*, 45.
(21) Yadav, J.; Rani, A.; Singh, V.; Murari, B. M. Prospects and limitations of non-invasive blood glucose monitoring using near-infrared spectroscopy. *Biomedical signal processing and control* **2015**, *18*, 214−227.
(22) Ballerstadt, R.; Gowda, A.; McNichols, R. Fluorescence resonance energy transfer-based near-infrared fluorescence sensor for glucose monitoring. *Diabetes Technol. Ther.* **2004**, *6*, 191−200.
(23) Lee, S. J.; Youn, B.-S.; Park, J. W.; Niazi, J. H.; Kim, Y. S.; Gu, M. B. ssDNA aptamer-based surface plasmon resonance biosensor for the detection of retinol binding protein 4 for the early diagnosis of type 2 diabetes. *Anal. Chem.* **2008**, *80*, 2867−2873.
(24) Elsherif, M.; Hassan, M. U.; Yetisen, A. K.; Butt, H. Wearable contact lens biosensors for continuous glucose monitoring using smartphones. *ACS Nano* **2018**, *12*, 5452−5462.
(25) Tseng, R. C.; Chen, C.-C.; Hsu, S.-M.; Chuang, H.-S. Contact-lens biosensors. *Sensors* **2018**, *18*, 2651.
(26) Chelliah, M.; Rayappan, J. B. B.; Krishnan, U. M. Synthesis and characterization of cerium oxide nanoparticles by hydroxide mediated approach. *J. Appl. Sci.* **2012**, *12*, 1734−1737.
(27) Shcherbakov, A. B.; Zholobak, N. M.; Ivanov, V. K. Biological, biomedical, and pharmaceutical applications of cerium oxide. *Synthesis, Properties and Applications* **2020**, 279−358.
(28) Xu, C.; Qu, X. Cerium oxide nanoparticle: a remarkably versatile rare earth nanomaterial for biological applications. *NPG Asia Mater.* **2014**, *6* (3), e90.
(29) Ngoc, L. T. N.; Bui, V. K. H.; Moon, J. Y.; Lee, Y. C. In-VitroCytotoxicity and Oxidative Stress Induced by Cerium Aminoclay and Cerium Oxide Nanoparticles in Human Skin Keratinocyte Cells. *J. Nanosci. Nanotechnol.* **2019**, *19*, 6369−6375.
(30) Balaji, S.; Mandal, B. K.; Vinod Kumar Reddy, L.; Sen, D. Biogenic Ceria Nanoparticles (CeO_2 Ps) for Effective Photocatalytic and Cytotoxic Activity. *Bioengineering* **2020**, *7*, 26.
(31) MacAdam, D. L. Photometric relationships between complementary colors. *J. Opt. Soc. Am.* **1938**, *28*, 103−111.
(32) Lee, S. H.; Cho, Y. C.; Choy, Y. B. Noninvasive self-diagnostic device for tear collection and glucose measurement. *Sci. Rep.* **2019**, *9*, 1−8.
(33) Zhang, Z. J.; Davidson, L.; Eisenbarth, G.; Weiner, H. L. Suppression of diabetes in nonobese diabetic mice by oral administration of porcine insulin. *Proc. Natl. Acad. Sci. U. S. A.* **1991**, *88*, 10252−10256.

https://doi.org/10.1021/acs.nanolett.1c01880
Nano Lett. 2021, 21, 8933−8940

(34) Tanaka, T.; Nabatame, H.; Tanifuji, Y. Insulin secretion and glucose utilization are impaired under general anesthesia with sevoflurane as well as isoflurane in a concentration-independent manner. *Journal of anesthesia* **2005**, *19*, 277−281.
(35) Windeløv, J. A.; Pedersen, J.; Holst, J. J. Use of anesthesia dramatically alters the oral glucose tolerance and insulin secretion in C57Bl/6 mice. *Physiol. Rep.* **2016**, *4*, e12824.
(36) Al-Rahayfeh, A.; Faezipour, M. Eye tracking and head movement detection: A state-of-art survey. *IEEE journal of translational engineering in health and medicine* **2013**, *1*, 2100212−2100212.
(37) LeBlanc, J. M.; Haas, C. E.; Vicente, G.; Colon, L. A. Evaluation of lacrimal fluid as an alternative for monitoring glucose in critically ill patients. *Intensive Care Med.* **2005**, *31*, 1442−1445.
(38) Peng, B.; Lu, J.; Balijepalli, A. S.; Major, T. C.; Cohan, B. E.; Meyerhoff, M. E. Evaluation of enzyme-based tear glucose electrochemical sensors over a wide range of blood glucose concentrations. *Biosens. Bioelectron.* **2013**, *49*, 204−209.
(39) Yan, Q.; Peng, B.; Su, G.; Cohan, B. E.; Major, T. C.; Meyerhoff, M. E. Measurement of tear glucose levels with amperometric glucose biosensor/capillary tube configuration. *Anal. Chem.* **2011**, *83*, 8341−8346.

https://doi.org/10.1021/acs.nanolett.1c01880
Nano Lett. 2021, 21, 8933−8940